

# Exclusive $\pi^0$ Muoproduction at COMPASS

Markéta PEŠKOVÁ<sup>1</sup>

(on behalf of the COMPASS Collaboration)

<sup>1</sup>*Charles university, Prague, Czechia*

*E-mail: marketa.peskova@cern.ch*

(Received January 14, 2022)

Hard Exclusive Meson Production and Deeply Virtual Compton Scattering (DVCS) are very promising reactions to study Generalized Parton Distributions (GPDs). Such exclusive measurements were performed at COMPASS in 2016 and 2017 after a short pilot run done in 2012 using the 160 GeV muon beams of both polarities at the M2 beamline of the CERN SPS. While exclusive  $\pi^0$  production is one of the main sources of background for DVCS measurement, it provides complementary information for parametrization of GPDs. We will report on results on exclusive  $\pi^0$  production cross section and its dependence on the squared four-momentum transfer and on the azimuthal angle between the scattering plane and the  $\pi^0$  production plane. This reaction is aiming to constrain the GPDs, in particular chiral-odd (“transversity”) GPDs.

**KEYWORDS:** GPD, COMPASS, exclusive  $\pi^0$  muoproduction

## 1. Introduction

The General Parton Distributions (GPDs) represent one of the most fundamental quantities for describing the 3D partonic structure of the nucleon [1–5]. GPDs correlate the information from Parton Distribution Functions (PDFs) and form factors, encoding the longitudinal momentum fraction and the transverse spatial position of a parton. They provide an access to the total angular momentum carried by a parton in the nucleon via the Ji’s relation [2]:

$$J^f(Q^2) = \frac{1}{2} \lim_{t \rightarrow 0} \int_{-1}^1 dx x [H^f(x, \xi, t, Q^2) + E^f(x, \xi, t, Q^2)]. \quad (1)$$

There are eight GPDs for each parton flavour  $q$ , four parton helicity-conserving (chiral even) GPDs,  $H^q(x, \xi, t, Q^2)$ ,  $\tilde{H}^q(x, \xi, t, Q^2)$ ,  $E^q(x, \xi, t, Q^2)$ , and  $\tilde{E}^q(x, \xi, t, Q^2)$ , and four corresponding parton helicity-flip (chiral-odd or “transversity”) GPDs:  $H_T^q(x, \xi, t, Q^2)$ ,  $\tilde{H}_T^q(x, \xi, t, Q^2)$ ,  $E_T^q(x, \xi, t, Q^2)$ , and  $\tilde{E}_T^q(x, \xi, t, Q^2)$ . Here,  $x$  denotes the average longitudinal momentum fraction of the struck quark with respect to the momentum of the nucleon target,  $\xi$  is half the change in the momentum fraction of the struck parton,  $t$  is the square of the four-momentum transferred to the target, and  $Q^2$  is the virtuality of the virtual photon  $\gamma^*$  exchanged between the lepton and the nucleon. The GPDs are expected to be universal quantities, i.e. to describe the nucleon structure independently on the experimental process. Most commonly used processes for GPDs parametrisation are Deep Virtual Compton Scattering (DVCS) and Hard Exclusive Meson Production (HEMP). DVCS is sensitive to GPDs  $H^q$ ,  $E^q$ ,  $\tilde{H}^q$ , and  $\tilde{E}^q$ . At leading-twist, the vector and pseudo-scalar meson productions by longitudinally polarised virtual photons are described by the GPDs  $H^q$  and  $E^q$ , and  $\tilde{H}^q$  and  $\tilde{E}^q$ , respectively. The contribution from transversely polarised  $\gamma^*$  in the exclusive  $\pi^0$  production

is expected to be suppressed by a factor of  $1/Q$  [6]. However, measurements of exclusive  $\pi^+$  production from HERMES [7] and the exclusive  $\pi^0$  production from JLab CLAS and Hall A [8, 9] have shown a significant contribution, which can be explained by a chiral-odd GPD coupling to a twist-3 wave function from GPD formalism of ref. [10]. In the framework of this phenomenological model the pseudo-scalar meson production is described by the GPDs  $\tilde{H}^q$ ,  $\tilde{E}^q$ ,  $H_T^q$  and  $\tilde{E}_T^q = 2\tilde{H}_T + E_T$ . Different partonic contents of the produced mesons provide different sensitivities to various GPDs. The exclusive  $\pi^0$  production, in particular, is sensitive to the chiral-odd GPD  $\tilde{E}_T^q$ . The recently published results from exclusive  $\pi^0$  production measurement at COMPASS, presented in this paper, support this finding [11].

## 2. COMPASS spectrometer set-up

COMPASS is a fixed-target experiment placed at the high-intensity M2 beam-line of the CERN Super Proton Synchrotron (SPS). It can accommodate both hadron and naturally longitudinally polarised  $\mu^+$  and  $\mu^-$  beams in the energy range between 50 and 280 GeV/c. For the GPD program the data were collected with the 160 GeV/c  $\mu^+$  and  $\mu^-$  beams with a polarisation of -0.8 and +0.8, respectively [12].

COMPASS is a two-stage magnetic spectrometer containing a tracking system with about 350 detector planes, a ring-imaging Cherenkov detector for particle identification, three electromagnetic and two hadronic calorimeters and two muon detectors. The GPD program started with a pilot run in 2012. The main data taking was carried out in 2016-17, collecting about nine times larger statistics than the pilot run. The COMPASS set-up has been complemented with a 2.5 m long liquid hydrogen target inserted in a proton recoil detector CAMERA, and a new electromagnetic calorimeter ECAL0. The 4 m long proton recoil detector consists of 2 concentric barrels with 24 scintillator slabs in each barrel and the proton detection is based on the time-of-flight between the two barrels. The ECAL0 calorimeter is situated right downstream from the target and allows to expand the accessible kinematic domain for DVCS and HEMP measurement towards higher  $x_B$ , improving the efficiency of detection of exclusive events and reducing the single-photon background from  $\pi^0$  and other decays. This set-up is capable of measuring the exclusive events within the kinematic domain from  $x_B \sim 0.01$  to 0.15, which is complementary to other experimental facilities.

## 3. Event selection

The event selection exploits the fact that the kinematics from the measured exclusive process  $\mu p \rightarrow \mu' p_{recoil} \pi^0$  is over-constrained. The  $\pi^0$  mesons are selected by their dominant two-photon decay. The event candidates contain two neutral clusters in the electromagnetic calorimeters, one reconstructed vertex inside the liquid-hydrogen target with an incoming muon and an identified outgoing muon, and a recoil proton candidate measured in CAMERA.

As the kinematics is over-constrained, for a given event, the measured quantities of recoil proton candidates are compared with the corresponding predictions obtained from the spectrometer information only. Figure 2 shows the result of such a comparison and the applied cuts for the selection of events using the data collected in the 2012 pilot run. The first left panel of fig. 2 shows the difference between the measured and the predicted value of transverse momentum  $\Delta p_T$ , and the second panel the difference of the azimuthal angle  $\Delta\phi$ . Here,  $p_T$  and  $\phi$  are considered in the laboratory

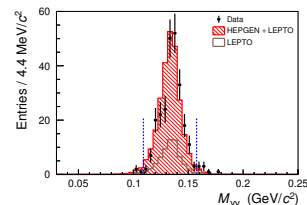


**Fig. 1.** Invariant mass of the  $\gamma\gamma$  system, and the  $2.5\sigma$  cut on the  $\pi^0$  mass [11].

system. Fig. 2 (third panel) represents the difference  $\Delta z$  between the longitudinal position of the hit in the inner CAMERA barrel  $z_A$  and the interpolated one using the interaction vertex position and the longitudinal position of the hit in the outer barrel  $z_B$ . Moreover the undetected mass:  $M_X^2 = (k + p - k' - q' - p')^2$  is constrained (see fig. 2, the rightmost panel), where  $k$  and  $k'$  denote the four-momenta of the initial and final muon, respectively;  $p$  and  $p'$  stand for the four-momenta of target and recoiled proton, respectively; and  $q'$  stands for the  $\pi^0$  four-momentum. Fig. 1 shows a  $2.5\sigma$  cut on the invariant mass of the double-photon system.

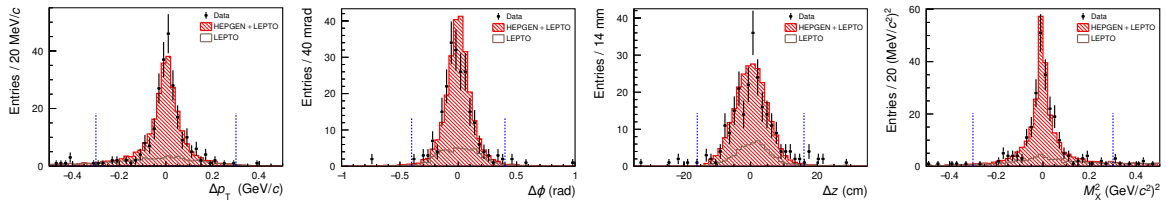


**Fig. 2.** Distributions of the exclusivity variables:  $\Delta p_T$  and  $\Delta\phi$  in the upper row, and  $\Delta z$  and the four-momentum balance in the lower row. The simulated non-exclusive  $\pi^0$  background is estimated using LEPTO (in brown), while the total  $\pi^0$  distribution is estimated using both LEPTO and HEPGEN (in red). Blue dotted vertical lines indicate the applied cuts [11, 13].

Main background to exclusive  $\pi^0$  muoproduction originates from non-exclusive deep-inelastic scattering (DIS) processes. The contribution of the background is estimated by Monte Carlo simulations. LEPTO generator is used to describe the distribution of the DIS background, and HEPGEN for modelling the exclusive  $\pi^0$  mesons. The signal and background reference samples with a wider kinematic range are used to normalise the simulations. Apart from wider kinematic range, signal sample was selected with the whole set of cuts as described above, while the background sample contains only events with more than one combination of vertex, cluster pair, and recoil proton candidate. The two reference samples described above are used to normalise the HEPGEN and LEPTO Monte Carlo yields on the experimental data using several kinematic variables. The sum of the respectively scaled HEPGEN and LEPTO fitted on the data is shown in fig. 3. The resulting fraction of non-exclusive (DIS) background is estimated to be  $(29^{+2}_{-6}|_{sys})\%$  [11].

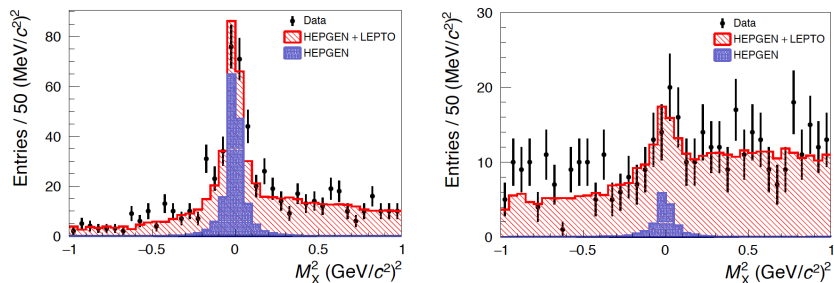


**Fig. 3.** Distributions of the undetected mass  $M_X^2$  for the signal (left) and background (right) reference samples as described in section 3 in the extended kinematic range, see details in ref. [11, 13]. Simulated data are shown in red (HEPGEN+LEPTO) and blue area (HEPGEN). Note that events with exclusive  $\pi^0$  topology have been removed from the LEPTO sample.

## 4. Results

The four-fold differential cross-section of the exclusive  $\pi^0$  production is obtained by correcting collected events for the luminosity<sup>1</sup>, the spectrometer acceptance, and a bin-wise background subtraction. The differential  $\mu p$  cross-section is extracted separately for  $\mu^+$  and  $\mu^-$  beams. The unpolarised cross-section is gained by averaging over the two beam polarities. The reduced  $\gamma^*p$  cross-section is derived from the unpolarised muon-proton cross section by using the transverse virtual-photon flux  $\Gamma = \Gamma(E_\mu, Q^2, \nu)$  [11]:

$$\frac{d^4\sigma_{\mu p}}{dQ^2 dt d\nu d\phi} = \Gamma \frac{d^2\sigma_{\gamma^* p}}{dt d\phi} \quad (2)$$

Here,  $\nu$  denotes the energy of the virtual photon  $\gamma^*$  and  $\phi$  the angle between the scattering and the hadronic plane. The reduced unpolarised exclusive  $\pi^0$  production cross-section then equals:

$$\frac{d\sigma^{\gamma^* p}}{dt d\phi} = \frac{1}{2\pi} \left[ \frac{d\sigma_T}{dt} + \epsilon \frac{d\sigma_L}{dt} \epsilon \cos(2\phi) \frac{d\sigma_{TT}}{dt} + \sqrt{2\epsilon(1+\epsilon)} \cos(\phi) \frac{d\sigma_{LT}}{dt} \right], \quad (3)$$

where  $\sigma_T, \sigma_L, \sigma_{TT}$ , and  $\sigma_{LT}$  are the structure functions,  $\epsilon$  is the virtual photon polarisation parameter. The subscript T(L) denotes the contribution from transversely (longitudinally) polarised  $\gamma^*$ , the subscripts TT and LT denote the contributions from the interference between transversely-transversely and longitudinally-transversely polarised photons. The structure functions from the formula (3) are connected to convolutions of GPDs with the individual hard scattering amplitudes, for details see e.g. [10, 11]. The  $\phi$ -dependence of the exclusive  $\pi^0$  cross-section average over the measured  $|t|$ -range as well as the  $|t|$ -dependence after the integration over  $\phi$  are presented in fig. 4.

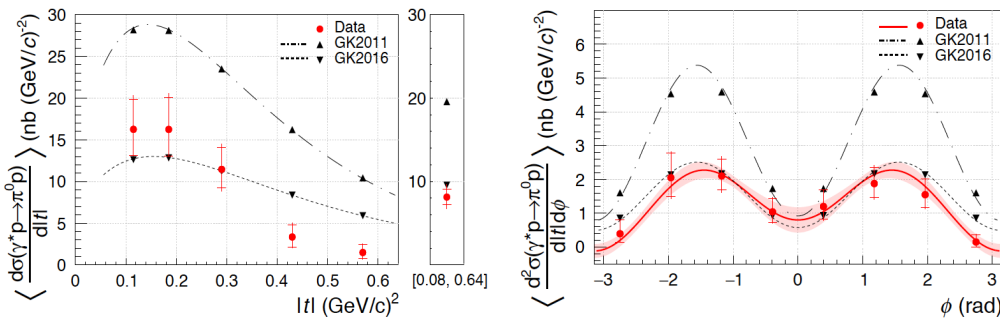


**Fig. 4.** **Left:** The exclusive  $\pi^0$  cross section as a function of  $|t|$ . **Right:** The exclusive  $\pi^0$  cross section as a function of  $\phi$ . Data are represented by the red dots, black dash-dotted line denotes the earlier Goloskokov-Kroll (GK) parametrisation [10], the dashed line represents the later version of the GK model adjusted to the new results [11, 14].

The analysis was performed on the final background-corrected data sample collected in the 2012 pilot run with average kinematics:  $\langle Q^2 \rangle = 2.0$   $(\text{GeV}/c)^2$ ,  $\langle \nu \rangle = 12.8$  GeV,  $\langle |t| \rangle = 0.26$   $(\text{GeV}/c)^2$ , and  $\langle x_B \rangle = 0.093$ . Our results are compared to the predictions of two versions of the Goloskokov-Kroll model, the dashed-dotted curve represents the prediction from an earlier version [10], while the dotted curve gives the later version [14]. The 2011 model was overshooting our result by approximately a factor two. However, it can be seen in fig. 4 that a difference in shape between the 2016 model and the data still remains. The red line in fig. 4

<sup>1</sup>Integral luminosity of the 2012 COMPASS measurement collected with  $\mu^+$  beam:  $L_{\mu^+} = 18.9 \text{ pb}^{-1}$ , and with  $\mu^-$ :  $L_{\mu^-} = 23.5 \text{ pb}^{-1}$

(right panel) shows a binned maximum-likelihood fit of the  $\phi$ -dependence of the exclusive  $\pi^0$  cross section to extract the different contributions according to eq. 3:

$$\frac{d\sigma_T}{dt} + \epsilon \frac{d\sigma_L}{dt} = (8.1 \pm 0.9^{+1.1}_{-1.0}) \frac{\text{nb}}{(\text{GeV}/c)^2} \quad (4)$$

$$\frac{d\sigma_{TT}}{dt} = (-6.0 \pm 1.3^{+0.7}_{-0.7}) \frac{\text{nb}}{(\text{GeV}/c)^2} \quad (5)$$

$$\frac{d\sigma_{LT}}{dt} = (1.4 \pm 0.5^{+0.3}_{-0.2}) \frac{\text{nb}}{(\text{GeV}/c)^2} \quad (6)$$

Results show a significant contribution of  $\sigma_{TT}$  and a small positive contribution of  $\sigma_{LT}$ . This supports the expectation that the exclusive  $\pi^0$  cross section should be dominated by transverse polarised virtual photon contribution, which indicates a strong effect of the chiral-odd GPD  $\bar{E}_T$ .

## 5. Outlook

The analysis of the COMPASS data collected in 2016/17 is currently ongoing. Over the two-year data-taking COMPASS collected about 9 times more statistics than in the 2012 pilot run. Fig. 5 shows the  $\gamma\gamma$  invariant mass distribution using a sample of the 2016 data, which are filtered using the aforementioned selections, this sample alone represents about 2.5 times larger statistics compared to the 2012 data. The first results of the exclusive  $\pi^0$  production cross-section from 2016, followed by the whole set of 2016/17, are expected to be released in foreseeable future, providing a further constraint for the Goloskokov-Kroll model.

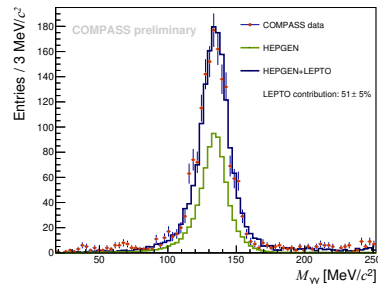


**Fig. 5.** Invariant mass of the  $\gamma\gamma$  distribution from the 2016 COMPASS data. The data (red points), are fitted with the sum of MC simulations, HEPGEN for signal and LEPTO for background (dark blue line). The HEPGEN sample is shown in green, scaled for its yield factor.

**Acknowledgments** This work is supported by Charles University in Prague, by the grant GAUK 60121, and the grant SVV No. 260576.

## References

- [1] D. Müller, D. Robaschik, B. Geyer, F. M. Dittes, and J. Hořejší, Fortsch. Phys. **42** 101 (1994)
- [2] X. D. Ji, Phys. Rev. Lett. **78** 610 (1997)
- [3] X. D. Ji, Phys. Rev. D **55** 7114 (1997)
- [4] A. V. Radyushkin, Phys. Lett. B **385** 333 (1996)
- [5] A. V. Radyushkin, Phys. Lett. D **56** 5524 (1997)
- [6] J. C. Collins, L. Frankfurt, and M. Strikman, Phys. Lett. D **56** 2982 (1997)
- [7] A. Airapetian, *et al.* (HERMES Collaboration), Phys. Lett. B **659** 486 (2008)
- [8] I. Bedlinskiy, *et al.* (CLAS collaboration), Phys. Lett. C **90** 025205 (2014)
- [9] M. Defurne, *et al.* (Hall A collaboration), Phys. Rev. Lett. **117** 262001 (2016)
- [10] S. Goloskokov, and P. Kroll, Eur. Phys. J. A **47** 112 (2011)
- [11] M. G. Alexeev, *et al.* (COMPASS collaboration), Phys. Lett. B **805** 135454 (2020)
- [12] F. Gautheron, *et al.* (COMPASS collaboration) CERN-SPSC-2010-014, SPSC-P-340 (2010)
- [13] M. Gorzellik, Cross-section measurement of exclusive  $\pi^0$  muoproduction and firmware design for an FPGA-based detector readout (University of Freiburg) doi:106094/UNIFR/15945 (2018)
- [14] S. Goloskokov, and P. Kroll, private communications (2016)